Motion Detection Circuits for a Time-To-Travel Algorithm

Rico Moeckel and Shih-Chii Liu

Institute of Neuroinformatics
University of Zürich and ETH Zürich
Winterthurerstrasse 190, CH-8057 Zürich, Switzerland
moeckel, shih@ini.phys.ethz.ch

Abstract—**We describe a new motion detection circuit that extracts motion information based on a time-to-travel algorithm. The front-end photoreceptor adapts over 7 decades of background intensity and motion information can be extracted down to a contrast value of 2.5%. Results from the circuits which were fabricated in a 2-metal 2-poly 1.5um CMOS process, show that the motion information can be extracted over 2 decades of speed.**

I. INTRODUCTION

One of the most researched monolithic neuromorphic chips described in the literature is motion sensors. The motion outputs of these chips are computed based on motion energy models, token-based models, correlation-based models, or optical flow models [1-8]. Some of the architectures are loosely based on the motion processing in insect visual systems [2] or that faithfully follows the neuronal circuits of the motion system [4, 5]. Many of these chips include front-end photoreceptor circuits that adapt to the background intensity [9] thus allowing the sensors to code motion over a wide range of background values.

There are many benefits to using these chips on a robotic platform for measuring image motion. The benefits of these sensors – *low-power consumption, parallel, collective computation, light weight* – make them attractive for mobile, battery-powered platforms, especially for autonomous micro-flying devices. These chips consume power in the order of µW while an equivalent implementation consisting of a silicon imager and a digital processor will consume at least 10 times more power. The area of the neuromorphic sensor is also much smaller than the latter, thus reducing the weight and size on the micro-flying robot. The models on which these chips are based provide for motion outputs that are invariant to a range of spatial and temporal frequencies in the image.

Neuromorphic motion sensors have been used for guiding the movement of a wheeled robot in a vision task [4, 10, 11] albeit in artificial lab environments with high contrast stimuli. There are only a handful of groups that have done some preliminary work in using neuromorphic sensors to guide the path of a micro-flying robot [12, 13]. The sensor described in [12] extracts information for controlling the altitude of unmanned aerial vehicles in open-sky environments. The chip contains several linear motion sensors laid out in an approximate circle so that the time-to-contact information can be extracted. The motion algorithm implemented on these sensors requires strong spatial derivatives and hence works best in environments with high contrasts.
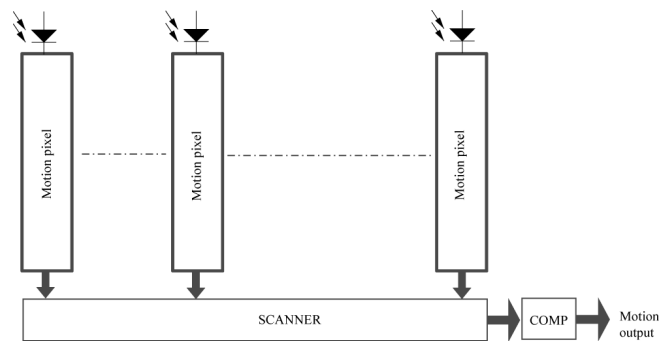

Figure 1. Block diagram of motion chip. Each pixel computes the local motion value using the facilitate-and-sample algorithm. The scanner circuit allows access to all pixels of the linear array and can be used to select the output from a certain pixel.

In this work, we describe a motion chip which is designed for a micro-flyer [14]. The circuit is based on the time-to-travel algorithm design implemented by Kramer and colleagues [2]. The motion is coded by measuring the time-to-travel of a pre-defined feature across 2 pixels.

There are three main differences in our circuits from the design in [2]. First, the pre-defined feature is detected through the use of 2 global thresholds. This allows us to reliably detect a feature in the presence of noise. Second, even though the system in [2] can measure a speed range

over 7 decades, the signal-to-noise (S/N) resolution of the motion output is not constant for all speeds because of the compressive encoding of the speed. Because the micro-flyer in [14] does not need such a large range of speed detection, we have altered the circuits to give us a higher S/N ratio for 2 decades of speed. Third, we included a scanner circuit which allows readout of local pixel information and we placed the motion comparator circuits after the scanner to reduce pixel mismatch. We first describe the chip architecture in Section II and we then show experimental results from the fabricated chip in Section III.

II. DESCRIPTION OF MOTION ARCHITECTURE

The architecture of the motion chip (Figure 1) shows the arrangement of the 24 motion pixels in a one-dimensional array. The different processing blocks in each motion pixel are shown in Figure 2. The basic structure of the motion pixel is based on the design in [2] which measures the motion using a facilitate-and-sample algorithm. A contrast edge falling on the photoreceptor (E) results in a voltage change in its output. The photoreceptor circuit [9] which is shown in Figure 3a has a high transient gain to temporal changes in intensity. Its output is processed by the LMC circuit [5] shown in Figure 3b. This circuit outputs a high gain, high-pass filtered version of the photoreceptor signal.
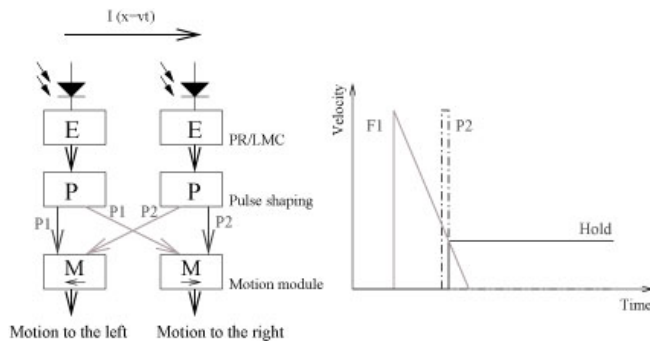

Figure 2. Schematic of the individual blocks in each motion pixel. The E block contains the photoreceptor and LMC circuit. Each P block creates a sampling pulse when the LMC output goes between 2 global threshold values. The sampling pulse (P2) resets a capacitor and samples the capacitor voltage (F1) of its neighboring pixel.

The LMC output is used to determine the presence of a pre-defined feature. A sampling pulse (P2 in Figure 2) is generated once the LMC output transitions between 2 global thresholds. This pulse is used to reset the voltage on the pixel's capacitor. It is also used to sample the voltage (F1 in Figure 2) on similar capacitors at neighboring pixels. Once the capacitor is pre-charged, the voltage decays at a linear rate which is adjustable through a bias. Depending on the time-to-travel of the feature between pixels, a sampled high voltage means that the time-to-travel was short and vice-versa.

The sampled values from the neighboring pixels are compared in the COMP block after the scanner (see Figure

1). The higher of the two values indicates the direction of motion. The combination of circuits in the motion pixel gives us a linear motion output that is somewhat invariant to changes in background intensity and contrasts. Local motion outputs are readout through a scanner.
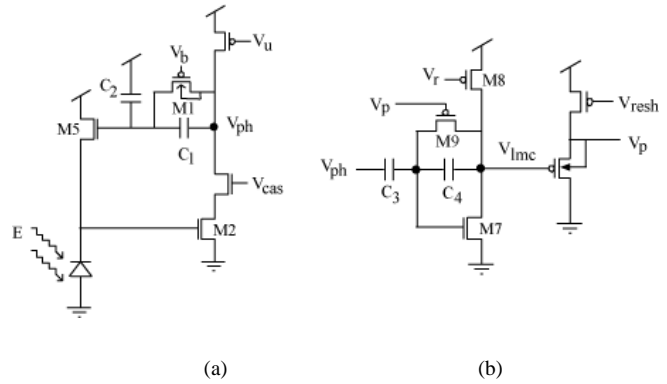

(a)   (b)

Figure 3. Circuits in the E block of Figure 2. (a) Photoreceptor circuit described in [9] The output, Vph has a high transient gain to temporal contrasts. (b) LMC circuit described previously in [5]. The LMC output has a reference value set by Vr.

III. EXPERIMENTAL RESULTS

A test chip was fabricated in a 2-metal 2-poly 1.5um CMOS technology. The size of the pixel is 54.4um x 1063.2um. The power supply is 5V. The stimulus for the experiments described here consists of drifting gratings on a passive LCD display. We varied the speed of the stimuli in the range of 0°/s to 100°/s which corresponds to the range of speeds that the motion chip would have to detect on the desired micro-flyer platform. Unless specified otherwise, the stimuli consist of sinusoidal gratings with a peak-to-peak contrast of 10%. The distance between the screen and the motion chip was 20cm and the focal length of the lens is 3.4mm.

A. Measured Outputs at a Pixel

We show the different output signals from a pixel in Figure 4. The feature detection signal Dthresh is generated once the LMC output has crossed from threshold 2 to threshold 1. The positive edge of Dthresh is used to create the sampling pulse P1 that also resets the voltage F1 on a capacitor. After the reset, F1 leaks away linearly. The pulse P1 is also used to sample the F1 signal from the left and right neighbors. The Hold signal shows the larger of these two sampled values. The use of the two thresholds for generating Dthresh makes the feature detection process very robust. If only a single threshold is used, the noise in the LMC output would trigger more than one event whenever the output was close to the threshold. The circuit would then detect non-existent features. Comparing the LMC output against two thresholds allows us to filter out this noise. Since we ensure that a new feature can only be detected when the LMC output is once more smaller than the two thresholds, only

noise whose amplitude is greater than the distance between the thresholds can trigger undesirable events. Thus we have for the following trade-off: A smaller threshold distance allows us to detect smaller changes in contrast but is more sensitive to noise. A bigger threshold distance allows a more robust operation in a noisy environment but we might miss features that could be detected with a smaller threshold distance.
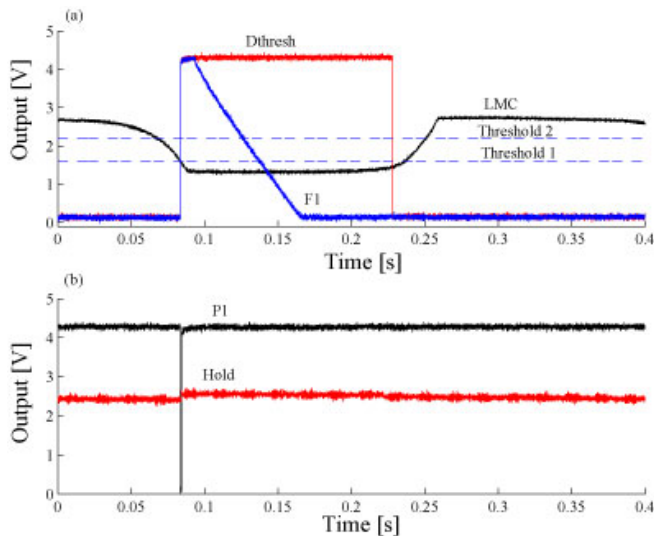

Figure 4.   Measured transient outputs from the fabricated chip. The LMC output is compared with the two thresholds. If it is below both thresholds, Dthresh is high showing that a feature is detected. This results in the generation of the sampling pulse P1 and the reset of the voltage F1 on the capacitor. P1 is used to sample the F1 signal from the neighboring pixels which results in the update of the Hold signal.
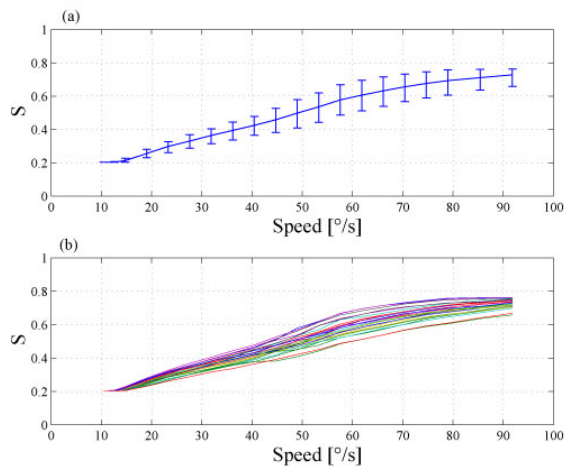

Figure 5.   Chip output S for bars moving from left to right. S=(1/(Vdd-V(Hold)). Due to offsets, S saturates at approximately 0.2 and 0.8. a) Global average of average response for all pixels. Error bars showing maximum and minimum average response. b) Average response of individual pixels.
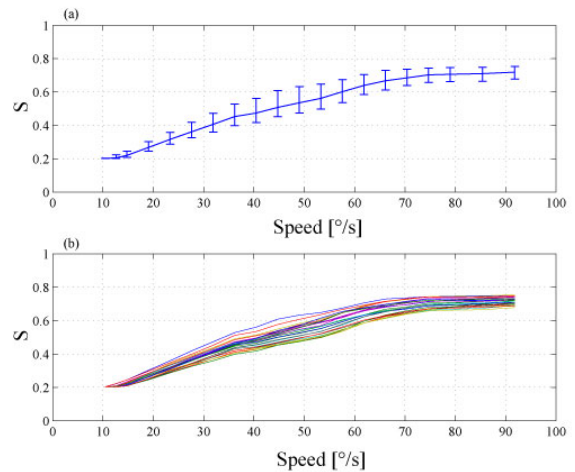

Figure 6.   Chip output S for bars moving from right to left. a) Global average of average response for all pixels. Error bars showing maximum and minimum response. b) Average response of all pixels.

B.   Dynamic Range

We measured the hold value of all pixels for a stimulus speed ranging from 0°/s to 100°/s. Figures 5 and 6 show how the signal S (computed from the Hold signal) varies as a function of stimulus speed for the two directions of motion. Ideally, the curves should be straight lines with the same slope, saturating at S=1 and with a deviation of 0. Because of offsets in the sampling and scanner buffer circuits, the output S saturates at 0.2 and 0.8 corresponding to 0V and 3.75V, respectively. The variation across all pixel responses for the same stimulus speed is primarily due to circuit mismatch. Additional noise comes from the power supply and crosstalk in the circuits but the biggest source of noise is the update frequency of the LCD display which we used for our stimulus. Nevertheless, Figures 5 and 6 show that we are able to cope with this noise and that we can extract motion information over 2 decades of stimulus speeds.

C.   Invariance to Contrast

Because of the LMC circuit and the 2 thresholds for defining a feature, our circuits can provide a constant motion output independent of contrast values down to 2.5%. The contrast is computed as follows: $C=(I_{max}-I_{min})/(I_{max}+I_{min})$ *100%, where I_{max} and I_{min} are the maximum and minimum intensity values of the stimulus as measured by a spotmeter. Figure 7 shows the peak-to-peak responses of the photoreceptor and LMC outputs and the Hold signal as a function of stimulus contrast for a single pixel. The signals were recorded in response to drifting gratings at 35°/s where the screen was 16cm away from the motion chip. Although the peak-to-peak amplitude of the photoreceptor and LMC signals decreased with decreasing contrast, the motion output was constant as long as the LMC peak-to-peak output is greater than both thresholds for the feature detection. The amplitude of the motion output of different pixels differs because of the noise described in the section before. However, using the same global threshold values for the

whole pixel array, all pixels can still operate down to a contrast value of 2.5%.
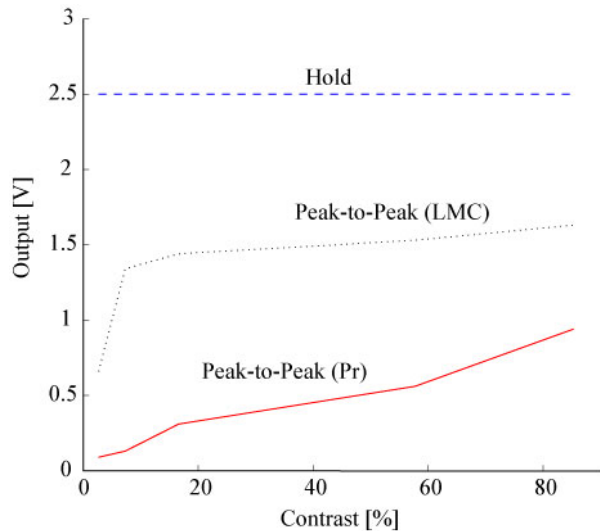

Figure 7. Invariance of the Hold motion output to different contrasts as measured from a pixel. Although the amplitude of the signals from the photoreceptor and the LMC drop with contrast, the Hold value stays constant down to a contrast value of 2.5%.

IV. CONCLUSION

In this paper, we describe a motion circuit that is based on a time-to-travel algorithm. The circuit is based on the architecture of [2] but has several differences which allow robust operation of this chip in the presence of noise. We can extract 2 decades of speed information for a fixed set of chip parameters. The results from this prototype are promising and the chip is now being extended to a larger array. Because of the pixel size, it would be impossible to go to a 2D architecture. We are currently exploring how to mount these linear arrays in a 2D configuration so that we can extract the necessary information for autonomous steering and altitude control. More importantly, we show that we can provide a robust motion output down to very low contrasts.

ACKNOWLEDGMENT

REFERENCES

[1] T. Delbrück, "Silicon retina with correlation-based velocity-tuned pixels", *IEEE Transactions on Neural Networks*, 4(3), pp. 529-541, 1993.

[2] J. Kramer, R. Sarpeshkar, and C. Koch, "Pulse-based analog VLSI velocity sensors", *IEEE Transactions on Circuits and Systems II*, 44, pp. 86-101, 1997.

[3] R. Etienne-Cummings, J. Van der Spiegel, and P. Mueller, "Hardware implementation of a visual motion pixel using oriented spatio-temporal neural filter", *IEEE Transactions on Circuits and Systems II*, 46(9), pp.1121-1136, 1999.

[4] R. Harrison and C. Koch, "A robust analog VLSI motion sensor based on the visual system of the fly", *Autonomous Robots*, **7**, pp. 211-224, 1999.

[5] S.-C. Liu, "A neuromorphic aVLSI model of global motion processing in the fly", *IEEE Transactions on Circuits and Systems II*, 47(12), pp. 1458-1467, 2000.

[6] A. Stocker, "An improved 2D optical flow sensor for motion segmentation", *Proceedings of the 2002 IEEE International Symposium on Circuits and Systems,* 2, pp. 332-335, 2002.

[7] V. Gruev and R. Etienne-Cummings, "Active pixel sensor with on-chip normal flow computation on the read out", *Proceedings of the 2004 11th IEEE International Conference on Electronics, Circuits and Systems*, pp. 215 – 218, 2004.

[8] S. Mehta and R. Etienne-Cummings, "Normal optical flow measurement on a CMOS APS imager", *Proceedings of the 2004 International Symposium on Circuits and Systems*, 4, pp. 848-851, 2004.

[9] T. Delbrück and C. Mead, "Adaptive photoreceptor circuit with wide dynamic range", *Proceedings of the 1994 IEEE International Symposium on Circuits and Systems*, 4, pp. 339-342, 1994.

[10] R. Etienne-Cummings, Viktor Gruev, and Mohammed Abdel-Ghani, "VLSI Implementation of Motion Centroid Localization for Autonomous Navigation," *Advances in Neural Information Processing Systems 11*, S. A. Solla, T. K. Leen and K.-R. Müller (Eds.), MIT Press, pp. 685-691, 1999.

[11] L. Reichel, D. Liechti, K. Presser, and S.-C. Liu, "Range estimation on a robot using neuromorphic motion sensors", *Robotics and Autonomous Robots,* 51(2-3), pp.167-174, 2005.

[12] M. Massie, C. Baxter, J. P. Curzan, P. McCarley, and R. Etienne-Cummings, "Vision chip for navigating and controlling micro unmanned aerial vehicle", *Proceedings of IEEE International Symposium on Circuits and Systems*, 3, pp. 786-789, 2003.

[13] W. Green, P. Oh, and G. Barrows, "Flying insect inspired vision for autonomous aerial robot maneuvers in near-earth environments", *Proceeding of the IEEE International Conference on Robotics and Automation,* pp. 2347-2352, 2004.

[14] J. C. Zufferey, A. Klaptocz, A. Beyeler, J. D. Nicoud, and D. Floreano, "A 10-gram microflyer for vision-based indoor navigation", *Proceedings of the IEEE/RSJ International Conference on Intelligent Robots and Systems (IROS' 2006)*, October 2006.